

Aftershock Fragility Curves and Tagging Assessments for a Mainshock-Damaged Building



M. Raghunandan & A.B. Liel

University of Colorado at Boulder, Boulder, CO USA

H. Ryu

Geoscience Australia, Canberra, ACT Australia

N. Luco

US Geological Survey, Golden, CO USA

S.R. Uma

GNS Science, Avalon, Lower Hutt, New Zealand

SUMMARY:

When multiple earthquakes occur within a short period of time, damage may accumulate in a building, affecting its ability to withstand future ground shaking. This study aims to quantify the post-earthquake capacity of a non-ductile 4-story concrete building in New Zealand through incremental dynamic analysis of a nonlinear multiple-degree-of-freedom simulation model. Analysis results are used to compute fragility curves for the intact and damaged buildings, showing that extensive damage reduces the structure's capacity to resist seismic collapse by almost 30% percent. The damage experienced by the building in mainshock, can be compared with the ATC-20 building tagging criteria for post-earthquake inspections, the purpose of which is to ensure public safety. Extensively damaged buildings, which are likely to be *red* tagged, pose a significant safety hazard due to decreased strength in future earthquakes. The effect of mainshock damage is also compared for multiple and simplified single-degree-of-freedom models of the same building.

Keywords: Aftershocks, Non-ductile concrete buildings, Collapse, Post-earthquake safety

1. INTRODUCTION

Buildings in seismically active regions may be at the risk of experiencing multiple earthquakes or mainshock-aftershock sequences in quick succession. Structures in Christchurch, New Zealand experienced such a sequence of earthquakes, when, first, a M_w 7.0 event in September, 2010, and, subsequently, a M_w 6.1 event in February, 2011, caused extensive damage to the built environment, much of which is still awaiting repair (Smyrou et al., 2011). The March, 2011 M_w 9.0 Tohoku, Japan earthquake was followed by hundreds of aftershocks as large as M_w 7.9, including at least 30 aftershocks greater than M_w 6.0 (USGS, 2011). Due to the close timing of these types of events, repair or retrofit activities are often not possible before the next earthquake, increasing the risk of further damage or collapse of already damaged buildings. The quantification of damage in buildings in earthquake sequences can equip us with the tools to mitigate the damage to the life and property as a result of better understanding of the building response and the building fragility in these events. Findings have important implications for post-earthquake inspections and building tagging procedures, which are intended to provide public safety after an earthquake.

There is significant ongoing research to understand the influence of mainshock-aftershock sequences and repeated earthquakes on steel and concrete buildings. A few of the studies have used nonlinear multiple-degree-of-freedom (MDOF) models to examine the response of steel structures (Fragiacomo et al., 2004; Lee and Foutch, 2004; Li and Ellingwood, 2007; Ruiz-García and Negrete-Manriquez, 2011), concrete bridges (Ruiz-García et al., 2008) and concrete frames (Hatzigeorgiou and Liolios, 2010) under earthquake sequences, while most other studies employed single-degree-of-freedom (SDOF) models (Sunasaka and Kiremidjian, 1993; Amadio et al., 2003; Hatzigeorgiou and Beskos,

2009; Hatzigeorgiou, 2010) for understanding structural behavior under earthquake sequences. Luco et al. (2004) proposed a probabilistic methodology to compute the residual capacity of mainshock-damaged buildings in terms of the ground motion intensity of an aftershock that can cause collapse or some other damage state. Using this methodology, Ryu et al. (2011) developed equations for building fragility in mainshock and aftershocks, implementing the procedure for SDOF analysis.

This study computes mainshock and aftershock building fragility curves of non-ductile concrete frame-type buildings, and relates the damage predicted to the building tagging criteria provided in documents available to assess the post-earthquake building safety, such as ATC-20 (ATC, 1989, 1995) and the New Zealand Society for Earthquake Engineering Building Safety Evaluation Guidelines. In ATC-20, rapid visual evaluations assign a building into three categories: 1) *green* tag or INSPECTED and safe to use, 2) *yellow* tag or RESTRICTED USE, *i.e.* requiring further detailed evaluation, or 3) *red* tag declaring building to be UNSAFE to occupy. These inspections take around 10-20 minutes per building, requiring a lot of time to inspect and tag all of the buildings in a region. The guidelines to describe the damage states are also qualitative and tagging decisions can vary depending on inspection personnel. For example, in ATC-20, a reinforced concrete frame building is to be tagged *red* if there is a collapse or partial collapse, or noticeable leaning in a building or individual story, or failure or incipient failure of columns, or serious degradation in column or beam elements, or severe panel zone cracking (ATC, 1989, ATC, 1995). The *red* tagging will be based on how severe the building inspector finds the building's condition. Probabilistic prediction of the probable damage during an aftershock on a typical building damaged during a mainshock, together with site-specific aftershock hazard information, will help in prioritizing regions for post-earthquake inspection. A more quantitative tagging criterion can provide clearer guidelines, eliminating a lot of *yellow* tagging in the process.

This paper describes the probabilistic methodology utilized to study the influence of the earthquake sequences on building capacity in the performance-based earthquake engineering framework. This probabilistic methodology utilizes nonlinear simulations of archetypical building models to assess the probable damage to the buildings subjected to multiple earthquakes. In this study, incremental dynamic analysis is carried out on the nonlinear MDOF analytical model of a typical non-ductile 4 story building in New Zealand, which is typical of structures built there in the 1960's or early 1970s. The building model is capable of capturing the critical aspects of strength and stiffness degradation of the building as the damage progresses, potentially leading to collapse. Nonlinear static pushover and dynamic analyses on the intact building are used to quantify the damage states thresholds, *i.e.* the displacement-based limits at which a particular damage state occurs. To quantify aftershock damage, the building is then subjected to a large number of earthquake sequences, such that the mainshock in the sequence brings the building into a particular damage state and the aftershock affects the damaged building. The damage observed in the intact buildings due to earthquake sequences can be linked back to the ATC-20 criteria for post-earthquake safety evaluation. Since the analysis of MDOF models subjected is computationally intensive, a similar analysis on a SDOF model calibrated to the same New Zealand building is conducted and results are compared.

2. BUILDING MODEL

Nonlinear dynamic analysis of mainshock-aftershock sequences is carried out on the numerical model of a typical 1960s era non-ductile 4-story New Zealand building. The non-ductile building model geometry, along with beam and column section and reinforcement properties, is shown in Fig. 2.1(a). These frames are potentially susceptible to brittle flexure-shear or shear-critical failure modes, due to low quantity and detailing of transverse reinforcement (typically spaced at 14 inches). The building has a flooring system prevalent in older New Zealand construction consisting of prestressed concrete ribs with permanent timber formwork and an in-situ concrete topping, supported by the building's primary beams. This floor system does not affect the strength of the beams (*i.e.* no slab effect). This flooring system results in significantly lower dead loads compared to a flat slab floor.

The analytical building model is implemented in *OpenSees* (2011), an open-source, object-oriented structural analysis platform developed by the Pacific Earthquake Engineering Research Center. The

building is modeled as a MDOF, two-dimensional, 3-bay frame. The building model uses lumped plasticity beam-column elements and inelastic joint shear springs to model nonlinear behavior of the materials, as well as bond slip between concrete and reinforcement. The hysteretic model developed by Ibarra et al. (2005) is used for plastic hinges in the beam-columns in order to simulate their degrading hysteresis behavior as the structure becomes damaged. The hysteresis modeling parameters are computed using the relations developed by Haselton et al. (2008), based on calibration of Ibarra model to 255 experiments on concrete columns. Geometric nonlinearity (*i.e.* P- Δ effects) in the building model is incorporated using a leaning column. The elastic properties of concrete sections are based on a cracked concrete section of 0.3 to $0.5EI_g$ depending on the axial load level in the element. The natural period of the building model is 1.40 s with ultimate base shear strength of 0.243 g and a ductility of around 3 (determined from pushover analysis). According to the 1965 New Zealand codes, this building would have been designed for a period of around 0.7 s and a base shear of $0.10g$. New Zealand engineers indicate that an overstrength factor (ratio of ultimate to design base shear) of about 2 is reasonable; the code period is typically an underestimate of building flexibility.

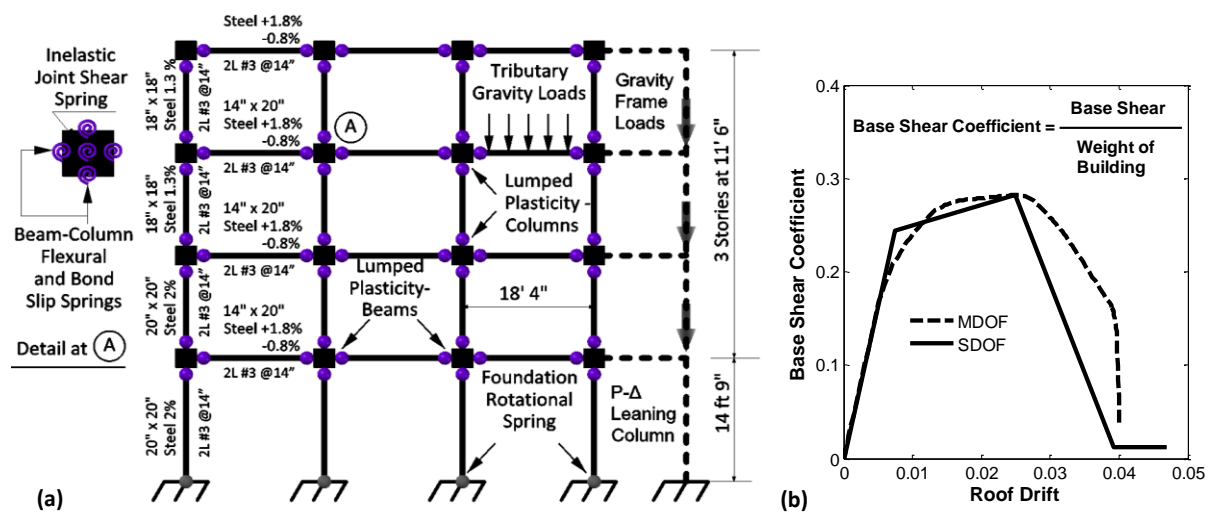


Figure 2.1 (a) Illustration of nonlinear MDOF building model, with reinforcement and member size design details; (b) Comparison of SDOF multilinear capacity curve with MDOF pushover analysis results.

In addition to the MDOF model, aftershock analysis is also conducted on an equivalent SDOF model of the same New Zealand building. The capacity curve for the SDOF is defined by a multilinear curve defined by three points corresponding to yield, ultimate and residual capacity, calibrated to the pushover curve of the more complex MDOF model. Fig. 2.1(b) compares the capacity curve of SDOF model with the pushover curve of MDOF. In addition to the capacity curve, to simulate the nonlinear hysteretic behavior of building model under dynamic loading, the model is assigned a moderate level of pinching and medium levels of cyclic deterioration, which are inputted in the Ibarra model (Ibarra et al., 2005).

3. DAMAGE STATES

During dynamic analysis, the building can undergo certain damage characteristics that are associated with significant changes in its strength and behavior. This building damage can be described by qualitative and quantitative descriptions of the discrete damage states: intact (undamaged), slight, moderate, less extensive and extensive. To quantify damage state thresholds for the structure, a nonlinear static pushover analysis is carried out on the analytical building model in *OpenSees* and the response of the structure at each step of the analysis is observed, as shown in Fig. 3.1(a). The four damage states are identified based on the initiation of distinct physical behavior in the structure and quantified by the maximum interstory drift ratio (across all the stories) at which that behavior is observed. The physical behavior associated with each of the defined damage states is reported in Table

3.1, and illustrated in Fig. 3.1(b). Table 3.1 also reports the maximum roof drift and residual interstory drifts observed at the onset of each of the various damage states during the pushover analysis. The damage state thresholds in terms of roof drifts are used to calibrate the SDOF model.

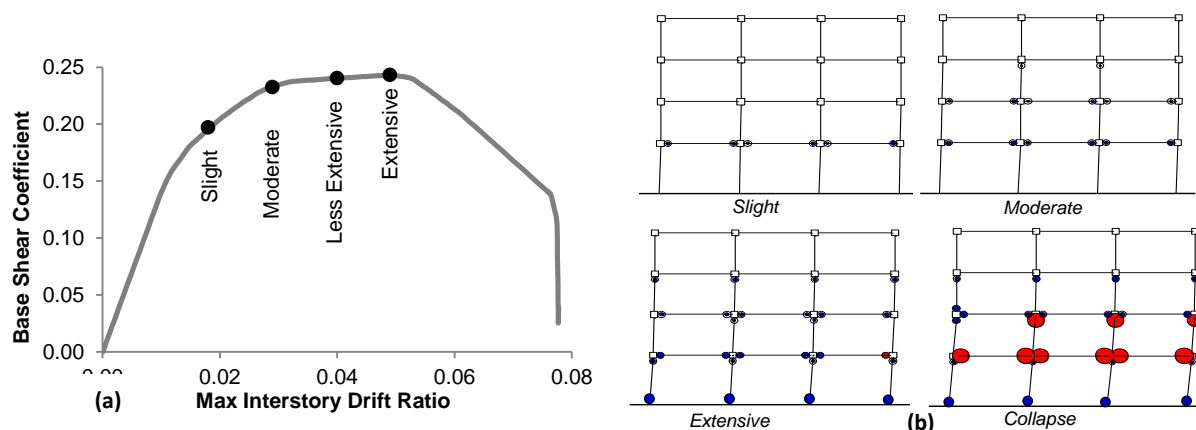


Figure 3.1 (a) Pushover analysis results for the building, showing the drift level thresholds associated with each damage state; (b) The physical state of building during each of the defined damage states.

This analysis assumes deterministic damage states, such that it is assumed that physical damage will occur during the dynamic analysis at the drift threshold defined for each damage state. In reality and as seen in dynamic analysis, depending on the characteristics of the ground motions, the physical damage states may not occur at the same interstory drift ratios as in the pushover analysis. Fig. 3.2(a) illustrates this variation in the drift levels at damage state initiation, where the labeled “individual IDA” correspond to the drift levels at which the physical states of slight, moderate, and extensive damage was observed during incremental dynamic analysis for each of 30 ground motions (Section 4.2). The drift thresholds identified in pushover analysis are very close to the median observed in dynamic analysis results. Similar relationships between median maximum roof drift from dynamic analysis and pushover analysis is also observed. Residual drifts are not used to define damage states, but are reported here because they may strongly influence structural behavior during the aftershock (Luco et al., 2004).

Table 3.1 Damage state descriptions, along with the damage state thresholds defined for the building.

Damage State	Physical Description	Max Interstory Drift	Roof Drift
Slight	Yielding of all beam hinges at one floor	0.018	0.009
Moderate	Start of yielding of columns	0.029	0.014
Less Extensive	Intermediate damage state ¹	0.040	0.020
Extensive	Plastic hinge rotation demand exceeding plastic hinge rotation capacity for at least one hinge in joint, beam or column	0.049	0.025
Collapse	Dynamic instability	0.12	0.060

¹ “Less Extensive” does not correspond to a specific physical state, but shows an intermediate state between Moderate and Extensive.

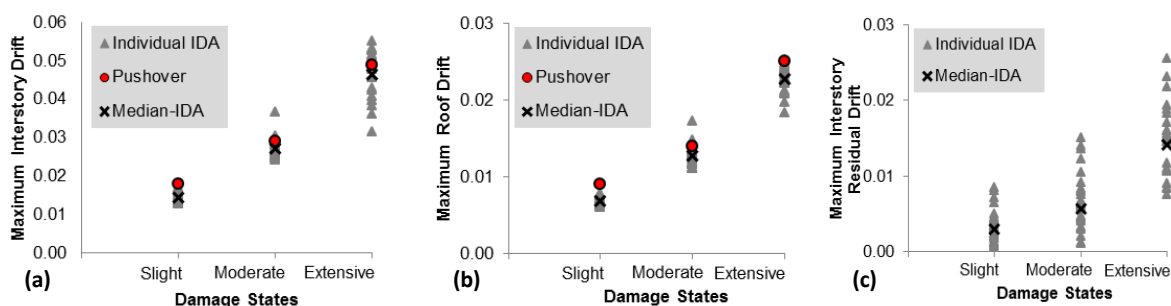


Figure 3.2 (a) Maximum interstory drifts, (b) roof drifts and (c) maximum residual interstory drifts associated with each damage state, as obtained from pushover and dynamic analysis.

4. NONLINEAR DYNAMIC ANALYSIS

4.1. Ground Motions

A set of 30 ground motions are used as both mainshock and aftershock records (Vamvatsikos and Cornell, 2006). These records are from California earthquakes with M_w between 6.5 and 6.9 and sites with closest distance to fault rupture within 15 to 33 km. Ground motions are recorded on firm soil with no directivity effects. The unscaled records have peak ground accelerations from 0.04 to 0.63g.

The ground motion intensity is measured using inelastic spectral displacement at the fundamental period of the structure, denoted S_{di} (Tothong and Cornell, 2006). Inelastic spectral displacement is defined as the peak displacement that a SDOF bilinear oscillator experiences when subjected to the ground motion. For this computation, the oscillator is assumed to have a 5% damping, and a pre-defined yield displacement (5.106 inches), which can be computed from the nonlinear pushover results (FEMA, 2009). The post-yield hardening stiffness for the oscillator is taken as 5% of initial stiffness. Research by Baker and Cornell (2006) has shown that structural response is significantly affected by ground motion spectral shape as well as spectral intensity. The conventionally-used intensity measure, elastic spectral acceleration, represents only spectral values at the fundamental building period. In fact, the spectral acceleration or displacement at many other periods becomes important for a building experiencing severely nonlinear behavior because its period elongates as damage occurs and the higher modes influence the response. S_{di} accounts for the longer natural periods as the bilinear oscillator yields and undergoes period elongation, thereby providing a simple measure for incorporating important spectral shape effects in addition to ground motion intensity.

4.2. Incremental Dynamic Analysis Procedure

To quantify the response of the building in the event of an earthquake or a sequence of earthquakes, incremental dynamic analysis (IDA) is carried out on the nonlinear building model *OpenSeesMP* (parallel version of *OpenSees*). In IDA, the nonlinear building model is subjected to a ground motion having a particular intensity (calculated here in terms of intensity measure S_{di}), and its response is recorded, including demand parameters such as maximum interstory drifts, maximum residual drifts or roof drifts (Vamvatsikos and Cornell, 2002). In subsequent analyses, the ground motion is scaled to a larger intensity and the nonlinear dynamic response again recorded. The process of repeated scaling of ground motions and dynamic analysis is continued until the structure collapses, which is indicated by dynamic stability (*i.e.*, very large interstory drifts, or roof drifts in case of SDOF). The incremental dynamic analysis process provides insights about structural behavior under rare, high-intensity ground shaking, for which few recordings are available. To account for the effect of record-to-record variability on structural response, IDA is repeated for each of the 30 ground motions in the set.

As the first step in the analysis, IDA is carried out on the nonlinear model of the intact New Zealand building, as illustrated in Fig 4.1(a); the bold (red) line highlights IDA results from one (of 30) ground motions. These results quantify the ground motion intensity the structure can withstand before experiencing a particular damage state. Due to differences in frequency content, duration and other ground motion characteristics, each ground motion is scaled to a different intensity before a particular damage level occurs; for example, depending on the ground motion, the building of interest reaches the moderate damage state (0.029 interstory drift) at S_{di} levels between about 5 and 9 inches (Fig. 4.1(a)). A fragility curve summarizes IDA results for each damage state, showing the probability of being in (or exceeding) a particular damage state as a function of ground motion intensity, as shown in Fig. 4.1(b). These fragility curves are computed based on the interstory drift damage state thresholds (Ryu et al. 2011). For example, Fig. 4.1(b) shows that the median S_{di} intensity necessary to cause at least moderate damage in the building is 7.62 inches. The standard deviation in the fragility represents differences in frequency content and other ground motion characteristics. For comparison purposes, Fig. 4.1(b) also shows fragility curves for the intact building obtained from the SDOF model. In most

cases the median capacities associated with each damage state are similar for the two models (1-11% different). However, the single-degree-of-freedom predicts smaller standard deviations, indicating that record-to-record variation is less significant for the simpler model.

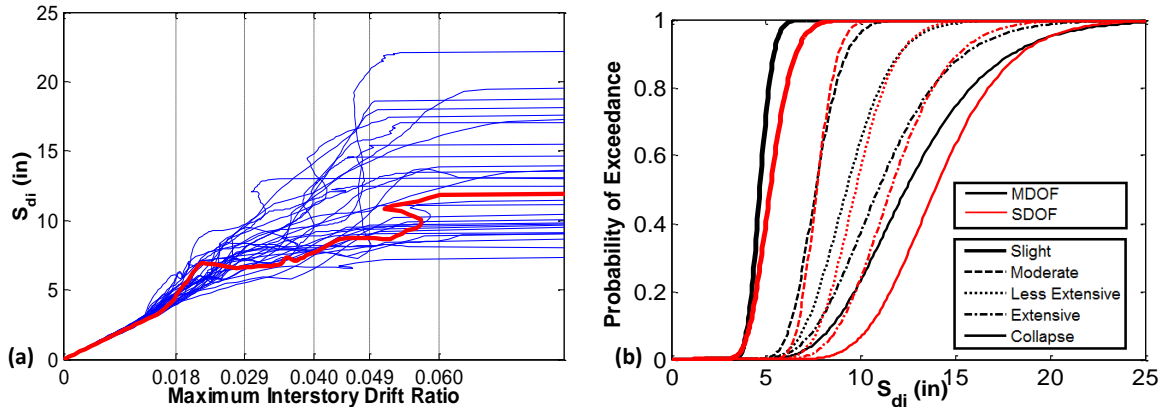


Figure 4.1 (a) IDA results (Note: the interstory drift values shown on the x -axis in Fig. 4.1 (a) correspond to the discrete damage states defined earlier); (b) Fragility curves for the intact New Zealand Building (black). The fragility curves for the intact SDOF model (red) are shown for comparison.

The aftershock analysis subjects the building to a mainshock-aftershock sequence, as shown in Fig. 4.2. The mainshock record is scaled to achieve a particular damage state in the structure and, subsequently, an aftershock record applied to the mainshock-damaged structure. A total of 900 earthquake sequences are created by combining each of the 30 mainshock ground motions with the same 30 ground motions applied as aftershocks. A rest period of four seconds is added between multiple earthquake events to recreate the real world situation, in which the structure comes to rest, but is not repaired. Dynamic analysis of the sequence is repeated with increasing scale factors applied to the aftershock record until the structure collapses, providing incremental dynamic analysis results for aftershocks. The aftershock response so obtained can be used to generate fragility curves for each damage state, but now conditioned on the damage experienced in the mainshock.

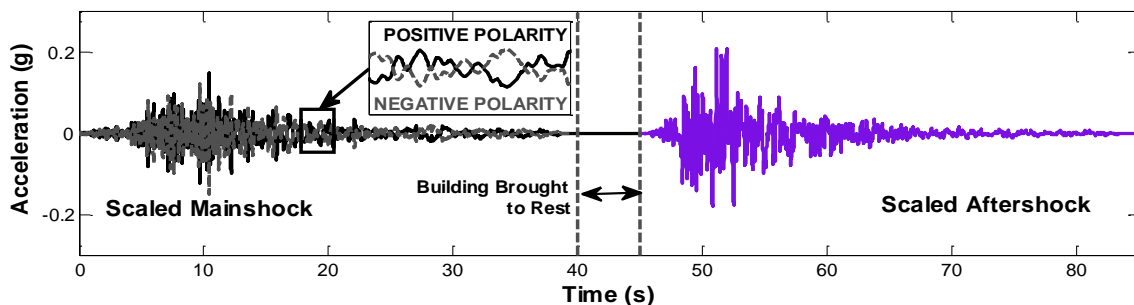


Figure 4.2 A mainshock-aftershock sequence for analysis of damaged building.

The issue of polarity of aftershock with respect to mainshock becomes important for cases where the residual drift after a mainshock is high (*i.e.* the structure is leaning to one side or another). The term “polarity” refers to the directions of the aftershock and mainshock, and specifically whether the aftershock is applied in the same direction or in the opposite direction as mainshock, tending to increase or reduce residual drift. To quantify the influence of polarity, polarities of the mainshock records were reversed in the analysis of both moderate and extensively damaged buildings.

5. RESULTS

The results obtained from incremental dynamic analysis of the mainshock-aftershock sequence are shown in Fig 5.1, where the x -axis represents the maximum interstory drift ratio experienced by the

structure during the aftershock (second ground motion in sequence). Results are shown for both (a,c) a building moderately damaged in the mainshock and (b,d) a building extensively damaged in the mainshock. The thick black line indicates the incremental dynamic analysis results from a particular mainshock-aftershock sequence. In the region shaded in grey, the interstory drifts undergone during the aftershock are smaller than those experienced in the mainshock and are not considered while calculating the damaged-building fragility because the damage state is unchanged from the mainshock. There is significant scatter in the intensity levels at which a particular damage state occurs for different aftershock records after the same mainshock record (Fig 5.1(a,b)). However, when the mainshock records are different, but the aftershock record is same (Fig 5.1(c,d)), the building exhibits similar behavior in the aftershock. This observation illustrates that the history of the path to the mainshock damage state is less important than the level of the building damage. However, Fig. 5.1(d) shows more variability than Fig. 5.1(c), indicating that as damage states become more severe, the increasing nonlinear behavior increases the variation in structural response.

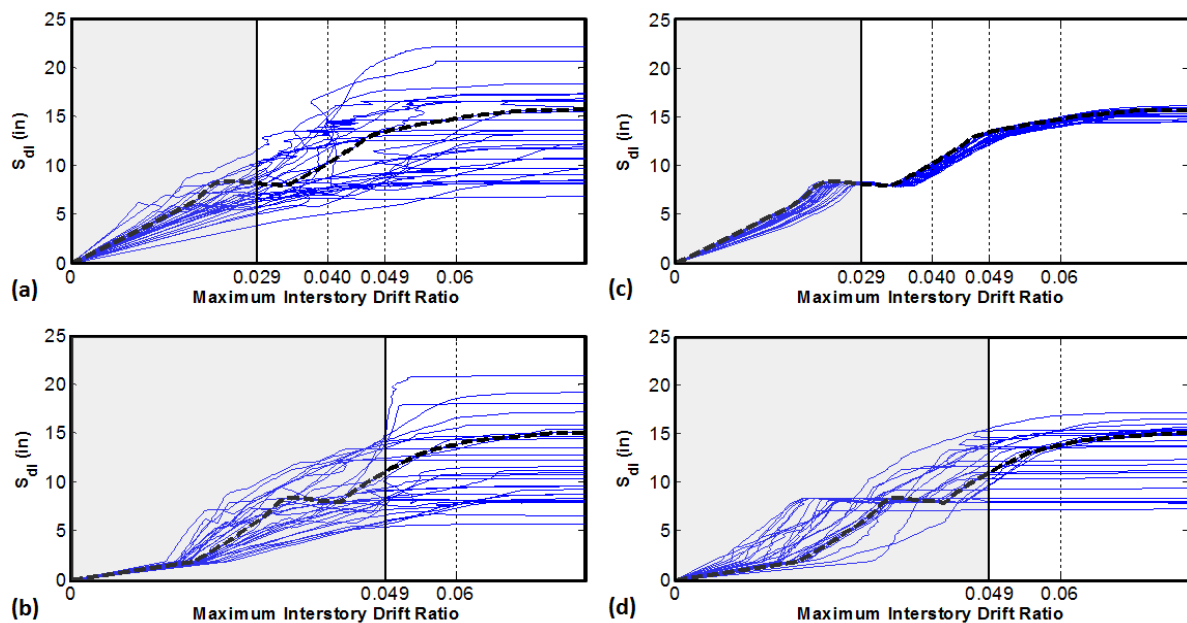


Figure 5.1 Incremental dynamic analysis results for the sequence where 30 different aftershock records were applied after experiencing either (a) moderate or (c) extensive damage in the same mainshock record; (b) and (d) show the behavior of the moderately and extensively damaged building, respectively, when subjected to sequences consisting of 30 different mainshock records, but the same aftershock record.

The dynamic analysis results from mainshock-aftershock sequences are used to compute the probability that a mainshock-damaged building will be in or exceed a particular damage state as a function of the aftershock shaking intensity (S_{di}), as shown by the fragility curves in Fig 5.2. After the aftershock record, the building will either remain in the mainshock damage state or transition to a worse damage state (the building cannot become less damaged). Fragility curves can be computed using the relations obtained from Ryu et al. (2011). The fragility curves calculated for buildings with moderate, less extensive and extensive damage in the mainshock are shown in Fig 5.2 (a,b,c), respectively, and compared with the the damage state fragility curves for the intact building. Moderate damage (Fig 5.2(a)) does not significantly change a building's fragility to aftershock records. However, the difference in fragility between the damaged and intact buildings increases significantly for less extensively and extensively damaged buildings (Fig 5.2(b) and (c)). As the building becomes more damaged in the mainshock record, the standard deviation (or dispersion) in the aftershock fragility also increases, indicating greater record-to-record variability in response.

The polarity of the mainshock-aftershock ground motion sequence does not impact the post-earthquake fragilities for a moderately damaged building, but it can become noticeable for the extensively damaged building. During the fragility curve calculations, the polarity effect is explored

using positive, negative, random, and minimum polarity. The minimum polarity case uses IDA results from the ground motion sequence which causes collapse at the lowest S_{di} , considering both positive and negative polarities. The median capacity associated with the extensive damage state is found to be around 5% lesser using the minimum polarity compared to others. The results here correspond to the positive polarity of ground motions, but for future analysis, random polarity is recommended, since the polarity of future records is unknown.

Results shown in Fig. 5.3 indicate that the calibrated SDOF model shows reasonable agreement with the MDOF model, both in terms of prediction of the fragility of the intact structure and in prediction of the reduction in capacity due to damage in the mainshock. The SDOF reduces computational time by a factor of around 160.

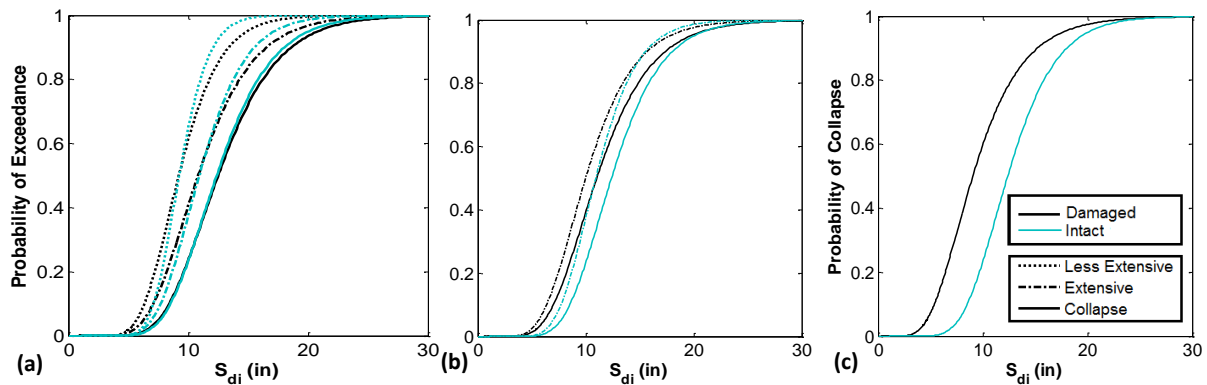


Figure 5.2 Fragility curves for building (a) moderately damaged in mainshock, (b) less extensively damaged in mainshock and (c) extensively damaged in mainshock (in black). The fragility curves for the undamaged (intact) building (blue) are shown for comparison.

To assess the performance of this non-ductile building during the 2010-2011 sequence of earthquakes in New Zealand, a nonlinear dynamic analysis is carried out on a set of recordings at 35 different sites in Canterbury from these two events (GeoNet, 2011a, 2011b). There are two horizontal components of ground motions recorded at each site for both the events, giving four possible earthquake sequences per site and, in total, 140 unique sequences. To consider the possibility that these independent events can occur in any order, 140 additional sequences are generated by reversing the order of two ground motions in the sequence. To explore the effects of stronger ground motions, all of the 280 sequences were multiplied by an arbitrary factor of 1.2, generating another set of 280 sequences. The damage state after the first event and the second event is observed and the transition probabilities between these events are illustrated in Fig. 5.4(a). Under the New Zealand sequences, the intact building is damaged to varying levels after the first event and, in some cases, further transitioned to a worse damage state after the second event. The median ground motion intensity associated with the onset of a particular damage state is calculated for the MDOF model subjected to New Zealand ground motions. These median capacities (called “New Zealand” results) are plotted in Fig. 5.4(b) along with the median capacities calculated for the MDOF subjected to the “general set” of records from Vamvatsikos and Cornell (2006). There is a decrease in the median capacity of the damaged building compared to the intact building on being subjected to New Zealand records, similar to what is observed for the general set of ground motions. On average, the median capacity of the structure using the New Zealand ground motions associated with each damage state is higher than for the general set, which may be due to different frequency content of the New Zealand ground motions. It is difficult to compare the damage seen in the actual New Zealand buildings during the earthquake sequences to the building damage in this study because the actual collapses occurred in buildings with different characteristics from our typical building. However, local failures similar to the extensive damage state were observed in a number of non-ductile buildings in New Zealand including beam-column joint failure, partial column failure etc. (EERI, 2011).

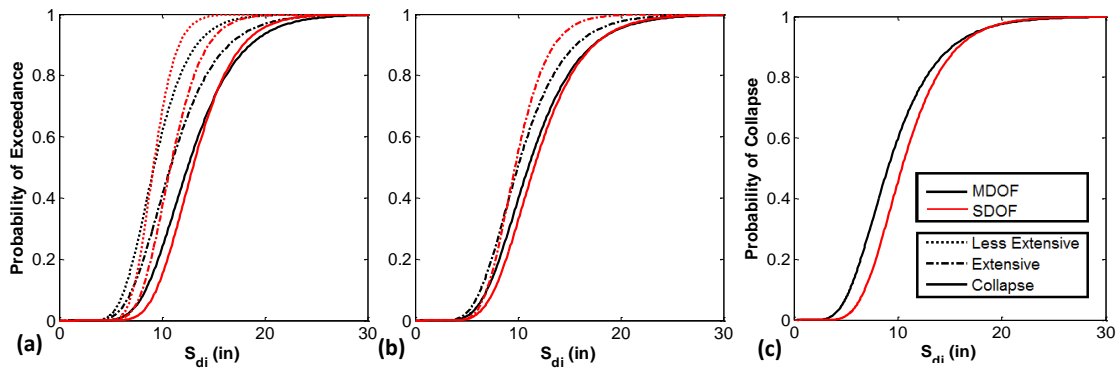


Figure 5.3 Fragility curves for SDOF model (red), when (a) moderately damaged in mainshock, (b) less extensively damaged in mainshock and (c) extensively damaged in mainshock. The fragility curves for the MDOF building (black) model are shown for comparison.

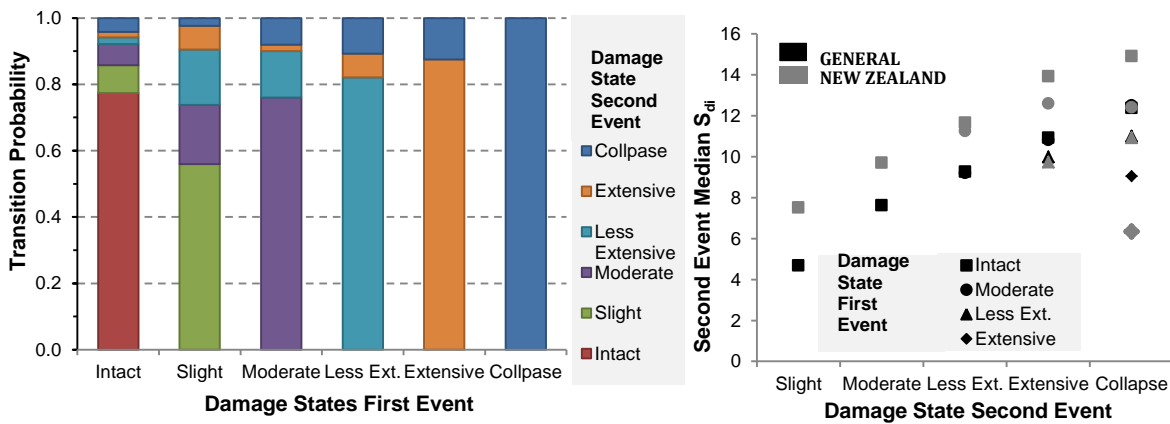


Figure 5.4 (a) Transition probabilities of the building from a particular damage state in first event to the damage state in second event for the New Zealand ground motions; (b) Comparison of the second event/aftershock median capacity for MDOF models using the general and New Zealand ground motions.

5. CONCLUSIONS

This study provides insight into the influence of earthquake sequences on building fragility. The moderately damaged building exhibits collapse capacity similar to an undamaged building, indicating that the building can be *green* tagged or in other words, is safe for use by its occupants. On the other hand, the building's ability to resist subsequent ground shaking decreases considerably when the structure is extensively damaged, and likely needs *red* tagging. The physical damage observed in the building during the extensive damage has description similar to the *red* tagged buildings in ATC-20, *i.e.* high interstory drifts, failure of any beam, column and joints hinges or local collapses. The results from a simplified SDOF system provides reasonable estimates median capacity of damaged and intact building, but exhibits lower standard deviation values because of less variability in damage propagation than a MDOF system. A similar analysis can be carried out on a suite of archetypical buildings prevalent in a region and building fragilities so computed for the intact and damaged buildings can be combined with the post-earthquake seismic hazard at site to prioritize regions for conducting post-earthquake inspections. These building curves also help to quantify the possible damage that may occur in buildings in a seismic region susceptible to multiple earthquakes from separate events.

ACKNOWLEDGEMENTS

Funding for this study comes from USGS cooperative agreement with the University of Colorado (Grant Number. G10AC00100). Conclusions and findings do not necessarily represent U.S. government policies.

REFERENCES

- Amadio, C., Fragiaco, M. and Rajgelj, S. (2003). The effects of repeated earthquake ground motions on the on-linear response of SDOF systems. *Earthquake engineering & structural dynamics*. **32: 2**, 291-308.
- ATC. (1989). ATC-20 Procedures for Postearthquake Safety Evaluation of Buildings. ATC
- ATC. (1995). ATC-20-2, Addendum to the ATC-20 Postearthquake Building Safety Evaluation Procedures. ATC
- EERI, 2011. Learning from Earthquakes -The M 6.3 Christchurch, New Zealand, Earthquake of February 22, 2011, EERI Special Earthquake Report.
- FEMA. (2009). Quantification of Building Seismic Performance Factors, FEMA.
- Frangiaco, M., Amadio, C. and Macorini, L. (2004). Seismic response of steel frames under repeated earthquake ground motions. *Engineering structures*. **26: 13**, 2021-2035.
- GeoNet. (2012a). Special processing for selected main-shock records from the Darfield Earthquake. ftp://ftp.geonet.org.nz/strong/processed/Proc/2010/09_Darfield_mainshock_extended_pass_band/
- GeoNet. (2012b). Special processing for selected main-shock records from the Christchurch Earthquake. ftp://ftp.geonet.org.nz/strong/processed/Proc/2011/02_Christchurch_mainshock_extended_pass_band/
- Haselton, C.B., Liel, A.B., Lange, S.T. and Deierlein, G.G. (2008). Beam-Column Element Model Calibrated for Predicting Flexural Response Leading to Global Collapse of RC Frame Buildings, PEER
- Hatzigeorgiou, G.D. (2010). Ductility demand spectra for multiple near-and far-fault earthquakes. *Soil Dynamics and Earthquake Engineering*. **30: 4**, 170-183.
- Hatzigeorgiou, G.D. and Beskos, D.E. (2009). Inelastic displacement ratios for SDOF structures subjected to repeated earthquakes. *Engineering Structures*. **31:11**, 2744-2755.
- Hatzigeorgiou, G.D. and Liolios, A.A. (2010). Nonlinear behavior of RC frames under repeated strong ground motions. *Soil Dynamics and Earthquake Engineering*. **30: 10**, 1010-1025.
- Ibarra, L.F., Medina, R.A. and Krawinkler, H. (2005). Hysteretic models that incorporate strength and stiffness deterioration. *Earthquake Engineering & Structural Dynamics*. **34: 12**, 1489-1511.
- Lee, K., Foutch, D.A. (2004). Performance evaluation of damaged steel frame buildings subjected to seismic loads. *Journal of Structural Engineering*, **130: 4**, 588-599.
- Li, Q. and Ellingwood, B.R. (2007). Performance evaluation and damage assessment of steel frame buildings under main shock–aftershock earthquake sequences. *Earthquake engineering & structural dynamics*, **36: 3** 405-427.
- Luco, N., Bazzurro, P. and Cornell, C. A. (2004). Dynamic versus static computation of the residual capacity of a mainshock-damaged building to withstand an aftershock. *13th World Conference on Earthquake Engineering*. Paper No. 2405
- OpenSees. (2012), “Open System for Earthquake Engineering Simulation. <http://opensees.berkeley.edu/>
- Ruiz-García, J., Moreno, J.Y. and Maldonado, I.A. (2008). Evaluation of existing Mexican highway bridges under mainshock–aftershock seismic sequences. *The 14th World Conference on Earthquake Engineering*. Paper 05-02-0090
- Ruiz-García, J. and Negrete-Manriquez, J.C. (2011). Evaluation of drift demands in existing steel frames under as-recorded far-field and near-fault mainshock–aftershock seismic sequences. *Engineering Structures*. **33:2**, 621-634.
- Ryu, H., Luco, N., Uma, S.R. and Liel, A. B. (2011). Developing fragilities for mainshock-damaged structures through incremental dynamic analysis. *9PCEE*. Vol. 225 1-8
- Smyrou, E., Tasiopoulou, P., Bal, İ.E., Gazetas, G. and Vintzileou, E. (2011). Structural and geotechnical aspects of the Christchurch (2011) and Darfield (2010) earthquakes In New Zealand. *Seventh National Conference on Earthquake Engineering*, Istanbul, Turkey.
- Sunasaka, Y. and Kiremidjian, A.S. (1993). A method for structural safety evaluation under mainshock–aftershock earthquake sequences, The John A. Blume Earthquake Engineering Center.
- Tothong, P. and Cornell, C. A. (2006). An empirical ground-motion attenuation relation for inelastic spectral displacement. *Bulletin of the Seismological Society of America*. **96: 6**, 2146–2164.
- USGS. (2012), United States Geological Survey. <http://www.usgs.gov/>.
- Vamvatsikos, D. and Cornell, C. A. (2006). Direct estimation of the seismic demand and capacity of oscillators with multi-linear static pushovers through IDA. *Earthquake Engineering & Structural Dynamics*. **35: 9**, 1097–1117.
- Vamvatsikos, D. and Cornell, C. A. (2002). Incremental dynamic analysis. *Earthquake Engineering Structural Dynamics*. **31 : 3**, 491–514.